Analysis of Strain Rate Impact on Makeup of Oilfield Premium Casing Connections

Jueren Xie

C-FER Technologies, Edmonton, Alberta, Canada

Abstract: This paper proposes a new approach for modeling connection makeup, using a material strain-rate dependant model. Abaqus analysis examples are presented to demonstrate the use of the proposed modeling approach. The impacts of strain rate on connection structural integrity and sealing capacity are discussed. The paper demonstrates that the proposed modeling approach provides a more accurate correlation to field and test data and presents a more realistic representation of connection behavior at makeup and under subsequent load conditions.

Keywords: Casing, Connection, Connection Torque Shoulder, Makeup, Makeup Torque, Static Loading, Strain-rate Dependence.

1. Introduction

The design of oilfield premium casing and tubing connections typically includes a form of buttress-type threads for the structural functions of the connection and a metal-to-metal radial contact section for sealability. Many premium connections also include an axial metal-to-metal shoulder next to the seal region of the pin and coupling design to control makeup, and in some designs, to gain additional sealability. Figure 1 shows a generic premium connection which employs buttress threads, a metal-to-metal radial seal and a pin-to-coupling shoulder.

Connection evaluation programs, usually consisting of a combination of finite element analysis (FEA) and physical testing, are often required to ensure structural integrity and sealing performance for field applications. FEA has becoming a more and more important component in the connection evaluation programs (Xie, 2009, and Xie and Tao, 2010).

Premium connections are often analyzed in two steps: makeup of connections and application of external loads. Appropriate modeling of connection makeup is crucial for the analysis but challenging to analysts. Static analysis modeling was typically used by analysts with consideration of the engagement of the threaded pin end into the coupling to the nominal makeup position by resolving overclosure interference between the threads of the pin and coupling, as well as in the radial seal and axial shoulder regions. However, field data of the makeup of premium connections suggests that while engagement of the threads and seals is developed gradually, engagement of the pin and coupling shoulders takes place in a fraction of a second. The impact of material strain rate due to the quick engagement of the pin and coupling shoulders is not considered in the static analysis, and as a result, the plastic deformation can be overestimated in the shoulder region, as well as causing potential numerical difficulties in the connection analysis.

This paper proposes a new modeling approach for connection makeup, by analyzing the connection material response using a rate-dependant material model. Using the Abaqus platform, analysis examples are presented to demonstrate the use of the proposed modeling approach. The impacts of strain rate on connection structural integrity and sealing capacity are discussed. The paper demonstrates that the proposed modeling approach provides a better comparison to field test data and presents what is believed to be a more realistic representation of connection behavior at makeup and under subsequent load conditions.

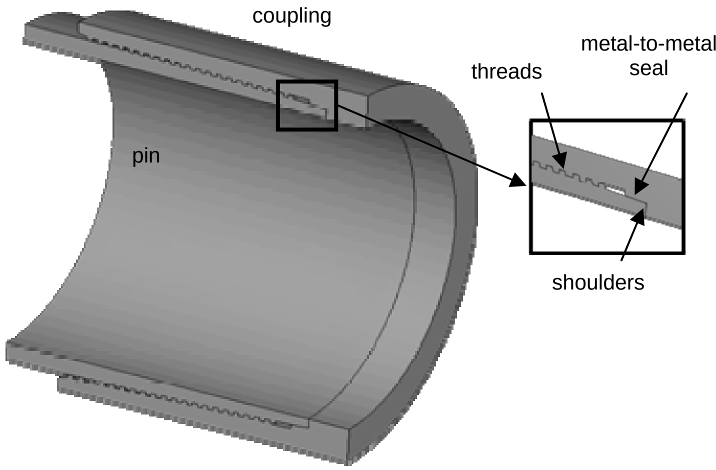

Figure 1. Schematics of a generic premium connection

2. Real-time observation of premium connection makeup

In the field and lab, tubular connections are typically made-up using a hydraulic power tong device. It is well recognized that makeup of connections, and in particular premium connections, requires careful control of torque and turns (position) during the screwing of the pin into the coupling. For premium connections with a torque shoulder, the torque-turn relationship before and after the shouldering point provides an important indication of the quality of the connection. Therefore, the makeup equipment is often combined with computer control and monitoring assemblies to generate a real time display of the makeup to accurately identify the sudden change in torque-turn slope indicating the point of shouldering and subsequent increased slope during shoulder engagement.

Several papers have discussed the controlled connection makeup procedures of the oilfield tubulars (Weiner and Sewell, 1967, Willis, 1983, Marojevic, 1986, Stewart, 1987, Raney et al, 1989, Tsuru et al, 1995). Figure 2 shows a typical torque-turn relationship for the makeup of a premium connection (Wills, 1983). It shows a correct makeup with a distinctive slope change where the torque shoulder engages.

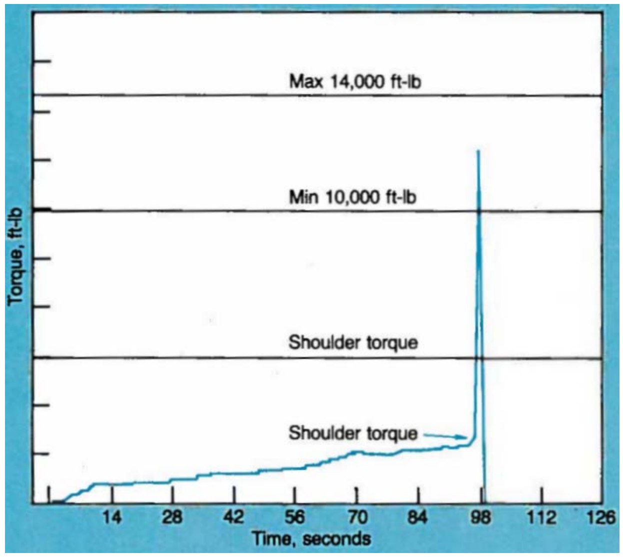

Figure 2. Typical makeup torque-turn relationship for a premium connection (Willis, 1983)

A schematic representation of torque-turn relationship for a premium connection is shown in Figure 3. The makeup of a premium connection can be characterized by three regions or stages:

1. Engagement of the thread and seal: thread and seal make-up, during which torque is applied to overcome pin-coupling thread interference and friction, up to a torque value designated as the shoulder torque, T_{sh}, at which the pin tip comes into contact with the coupling torque shoulder;
2. Engagement of the pin-coupling shoulders: further advancement of the pin into the box causes force to be developed between the pin and coupling components at the shoulder and reacting thread interfaces, causing an incremental torque ΔT that is a function of the number of incremental turns after shouldering, $\Delta turn$; and
3. Release of the applied make-up torque.

As such, the torque-turn relationship for a premium connection can be characterized by the following four key parameters:

T_{sh} = Torque value at shouldering;

T_{max} = Final torque after shouldering, which is the sum of the torque at shouldering, T_{sh}, and the incremental torque, ΔT, post shouldering;

$turn_{sh}$ = Turn value at shouldering; and

$\Delta turn$ = Turn increment from shouldering to release of torque.

The values of these four parameters vary with the size, weight and grade of the tubular and the design of the connection. However, the values of these makeup parameters are often controlled to the acceptable ranges to ensure proper make-up. For example, one connection supplier (TenarisHydril,2011) listed several rejection criteria, including values of high or low final torque, high or low shoulder torque, and apparent non-linear torque increase after shouldering (indicating connection yield). For many connections of typical casing sizes (e.g. 177.8 mm to 244.5 mm), the turn increment ($\Delta turn$) can be around 0.05 turns, and the makeup speed can be in the range of 4 to 7 RPM (Rotations Per Minute).

For most premium connections, the torque-turn relationship during the incremental turns following shouldering shows a primarily linear response. This $\Delta T - \Delta turn$ response is an important indication of the quality of the connections and is therefore a key design consideration and is as well used for makeup control while limiting the plastic deformation in the shoulder during makeup.

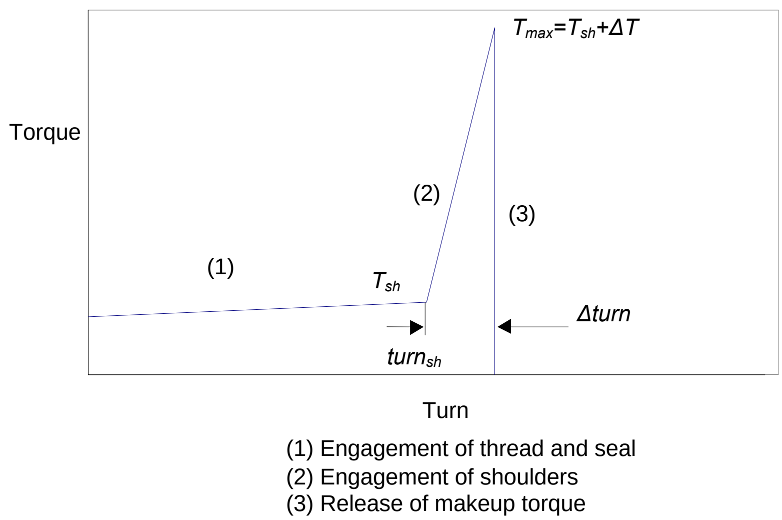

Figure 3. Schematic representation of torque-turn relationship

3. Modeling of connection makeup

3.1 Structural and material models

Figure 4 shows a schematic representation of the finite element model for a premium connection and a section of the pipe body. Due to the symmetry of deformations about the connection centre under the imposed loading conditions, only one half of the coupling was modeled. At the coupling centre plane (A-A), symmetric boundary conditions were assumed.

To analyze the structural and sealability behaviour of a premium connection, a finite element model of the half coupling and casing section can be created using axisymmetric solid elements (e.g. CAX4 in Abaqus) or generalized axisymmetric solid element (e.g. CGAX4). Connection makeup can be modeled as axisymmetric loading and symmetric boundary conditions can be assumed for both ends of the models. To assess the behaviour of connections subjected to non-axisymmetric loads, such as those resulting from bending induced by wellbore curvature, casing buckling and formation shear movement, axisymmetric elements with nonlinear asymmetric deformation (e.g. Abaqus CAXA4N elements) can be used (Xie, 2007).

For the analysis example presented in this paper, Grade 80 steel (i.e. nominal minimum yield strength of 80 ksi (552 MPa)), which is a commonly used oilfield tubular material, was modeled using an elastic-plastic, isotropic hardening constitutive relationship. The Young's modulus was assumed to be 200 GPa, the static yield strength was assumed to be 552 MPa, and the post-yield behaviour with material strain-hardening was modeled.

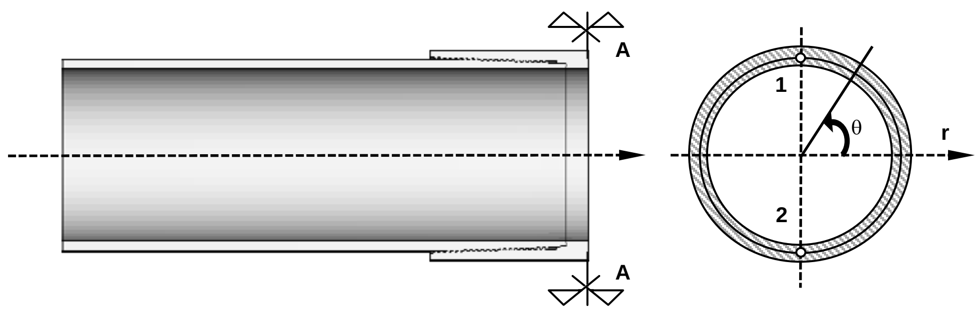

Figure 4. Section of coupling and casing pipe body modeled

3.2 Static analysis model

A static model has been widely used for analyzing connection makeup and was considered for comparison with the results of a strain-rate dependent model. In the static analysis, it was assumed that a premium connection was made up at a very slow strain rate (i.e. strain-rate independent), and therefore, the static yield strength properties were used for the material constitutive model. The makeup torque effects on the connection were modeled by analyzing the interference fit in the thread, seal and shoulder regions, in two distinct steps:

1. interference fit in the threads and seal; and
2. interference fit in the shoulder.

Note that although Figure 3 shows three load steps during the connection makeup, the third step (i.e. release of torque) can be ignored in a static analysis mode, assuming the normal contact stress conditions between pin and coupling components remain unchanged after the second step.

The interference values in the threads and seal are specified by connection design. For the representative premium connection considered for this assessment, the shoulder interference was calculated based on the geometry of the selected connection design and the turn increment (*Δturn*) introduced after the shoulder torque position:

$$I_{sh} = pitch \times \Delta turn$$

where *pitch* is the average distance between neighbouring threads for the pin and coupling.

Note that the above equation assumes that the axial pin displacement corresponding to the incremental turn value (and associated incremental torque) is fully accommodated by interference at the shoulder interfaces. Also, parametric finite element analyses established that the pin and box twist angles that develop over the thread and seal regions in response to reasonable makeup torque and friction values are insignificant compared to the typical incremental turn values.

3.3 Strain-rate dependent analysis model

As discussed in Section 2, connection makeup is a time-dependent process. For example, at a makeup speed of 6 RPM, it takes 0.5 seconds to load the shoulder with the incremental rotation following shouldering of approximately 0.05 turns. If the shoulder engagement will introduce 5% of equivalent plastic strain in the shoulder (typical of oilfield casing connections of the type and tubular material considered here), the average strain rate over this period would be approximately 10% per second. This high strain rate would introduce an increase in the material yield strength. Figure 5 shows the impact of strain rate on mild steel's yield and tensile strength properties (Manjoine, 1944). At the strain rate of 10%/second, Figure 5 indicates that the yield strength can increase by approximately 30%.

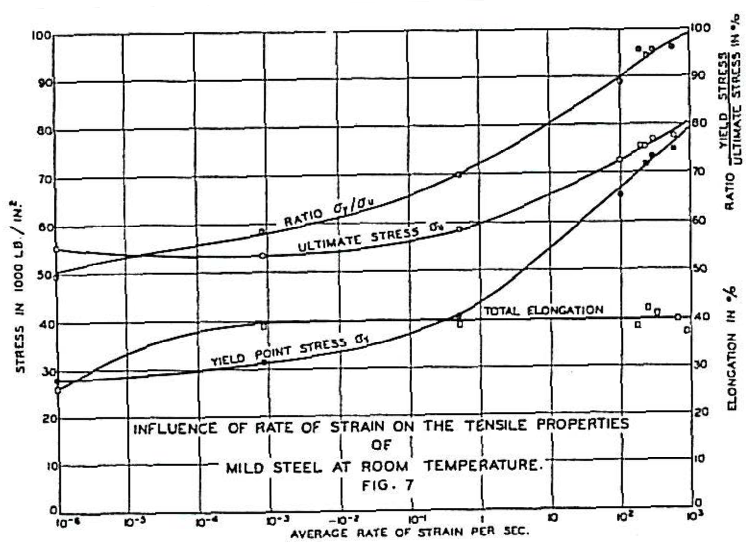

Figure 5. Influence of strain rate on tensile properties of mild steel at room temperature (Manjoine, 1944)

The effect of strain rate on the elastic-plastic response of the material can be considered using the following overstress power law (Ting, 1961):

$$\dot{\bar{\varepsilon}}^{pl} = D\left(\frac{\bar{\sigma}}{\sigma_0} - 1\right)^{p}$$

in which $\dot{\bar{\varepsilon}}^{pl}$ is the equivalent plastic strain rate, $\overline{\sigma}$ is the yield stress at a nonzero plastic strain rate, σ_0 is the static yield stress, and *D* and *p* are material parameters defining the overstress power law, which were set as *D* = 20 and *p* = 6 based on the experimental results of mild steel by Manjoine (1944).

Abaqus provides the capability to model the above equation for strain-rate effect which was described as the hardening dependencies with an overstress power law (Abaqus, 2010).

In the strain-rate dependent analysis, the connection makeup was modeled in three distinct steps:

1. interference fit in the threads and seal;
2. interference fit in the shoulder; and
3. release of torque.

Note that in the first and second steps of interference fit in the threads, seal and shoulder, the loading was applied at a high rate generated by the specified makeup speed and connection geometry. For the third step (i.e. release of torque), the loading was modeled at zero speed, i.e. a static loading with infinite time period. As such, the static material properties were used for the third loading step.

4. Analysis example

An analysis example is presented here to demonstrate the response of connection makeup on the structural and sealability of a premium connection using the static and strain-rate dependent models. The analysis example considered a 244.5 mm, 59.5 kg/m Grade 80 generic premium connection. This generic premium connection model included the basic features common to the premium connections currently used in high temperature thermal well applications (e.g. buttress threads, axial torque shoulders, and radial metal-to-metal seals) such that the analysis results were representative of such connections. Note that the generic premium connection model presented here should not be taken as being representative of any specific commercially available connection product. It is also important to note, however, that premium connection designs must be modeled based on the proprietary design details of the connection.

The generic premium connection design was assumed to be subjected to 0.05 incremental turns following shouldering, and the makeup was modeled at a speed of 6 RPM. Therefore, the incremental turns would be completed in 0.5 second.

Figure 6 presents the torque-turn relationships following shouldering based on the static and strain-rate dependant models. In establishing torque values, a friction coefficient of 0.025 between the pin and coupling interfaces was used in the incremental turn analysis.

As shown in Figure 6, both static and strain-rate dependent models start with a small slope increase (i.e. from 0 to about 0.01 incremental turns) in the torque-turn curves due to the redistribution of contact stress between pin and coupling in the thread and seal regions. Following this initial slope increase, the static model shows a linear increase in torque to approximately 0.035 turns beyond which the slope of the torque-turn response start to decrease. For the strain-rate dependent model, Figure 6 shows that the torque-turn relationship is primarily linear over the region from 0.01 to 0.05 incremental turns.

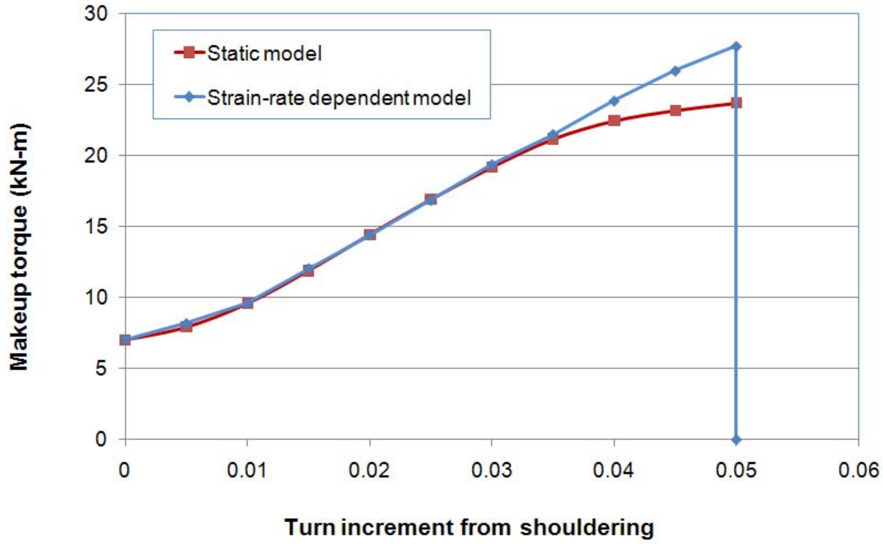

Figure 6. Analysis results of torque-turn relationships based on static and strain-rate dependent models

Figure 7 presents the analysis results of axial stress, effective stress and equivalent plastic strain at end of the applied incremental turns based on the static and strain-rate dependent models. The strain-rate dependent model shows significantly higher axial compressive stress in the shoulder region, and as a result, significantly higher effective stress as compared to that from the static model. However, the strain-rate dependent model also shows a more limited yield zone with lower plastic strain magnitude as compared to the static model.

Figure 8 presents the maximum plastic strain in the shoulder region over the applied incremental turns based on the results from analysis using the static and strain-rate dependent models. For the static model, as noted above, the connection makeup was modeled in two steps: interference fit in threads and seal, and interference fit in shoulder. In the second step, Figure 8 shows that the plastic strain increased gradually from 0.01 to 0.035 turns. However, after 0.035 turns, significant plastic strain developed in the static model. The plastic strain magnitudes were 6.1% and 20.7%, respectively, at 0.035 and 0.05 turns for the static model. Note that, as shown in Figure 6, the slope of the torque-turn relationship starts to decrease at approximately 0.035 turns for the static model.

For the strain-rate dependent model, also noted above, the connection makeup was modeled in three steps: interference fit in threads and seal, interference fit in shoulder, and release of torque. In the second step, Figure 8 shows that the plastic strain in the shoulder increased gradually over the region from 0.01 to 0.05 turns with the maximum magnitude of 7.9% at the end of the second make-up step. However, during the third step (i.e. release of torque), the plastic strain increased to 14% due to the change in loading rate (i.e. strain rate) from the very high rate in the second step to static loading condition of the third step. Nonetheless, Figure 8 shows that the final maximum plastic strain of 14% from the strain-rate dependent model is significantly lower than that from the static model.

Based on the analysis results, it can be concluded that the difference in the torque-turn relationships appears to come from the difference in the extent of the yield zone and the magnitude of plastic strains generated in the static and strain-rate dependent models. The static model appears to overestimate the magnitude of the plastic strain and the extent of the yield zone. As a result, the static model was unable to predict the primarily linear response of torque-turn relationship as observed in the field and lab (see Figures 6, 2 and 3). On the other hand, the strain-rate dependent model showed a more limited yield zone with less plastic strain in the shoulder region, and it was able to capture the primarily linear response of the anticipated torque-turn relationship.

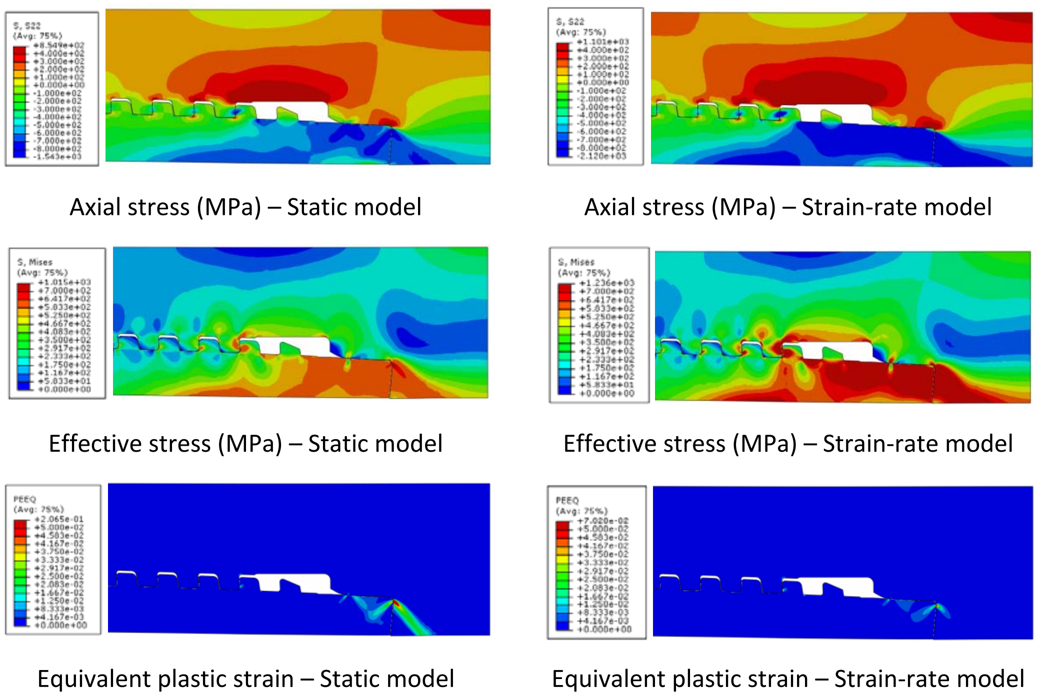

Figure 7. Contour plots of axial stress, effective stress and equivalent plastic strain in the shoulder region based on static and strain-rate dependent models

Figure 9 presents the profile of seal contact stress after makeup for the two connection models, which is another key result from the makeup analysis. The static and strain-rate dependent models show similar contact stress distributions in the seal region. The seal contact intensity values, defined as the integration of seal contact stress over the effective seal length (which is half of seal length away from the pin tip), are 670 and 665 N/mm for the static and strain-rate dependent models respectively. These results suggest that the final seal contact profiles were not affected by the loading rate.

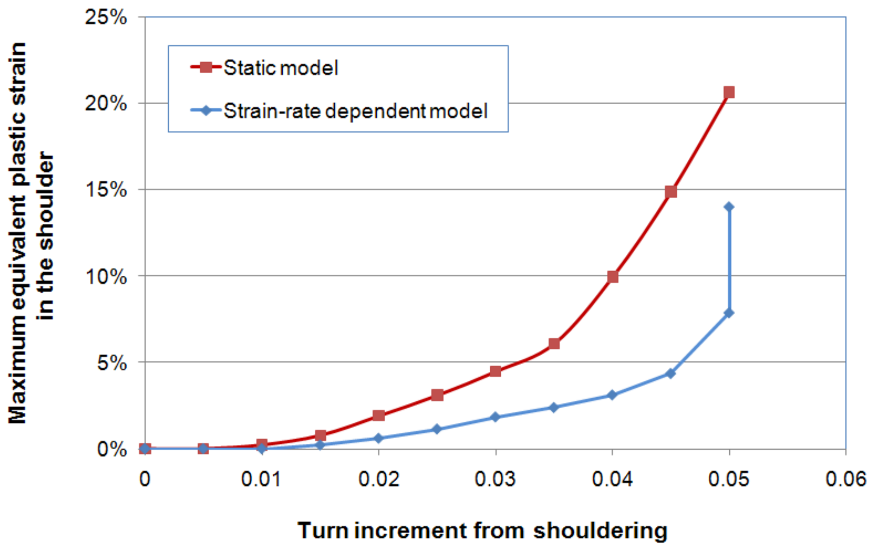

Figure 8. Analysis results of maximum equivalent plastic strain in the shoulder based on static and strain-rate dependent models

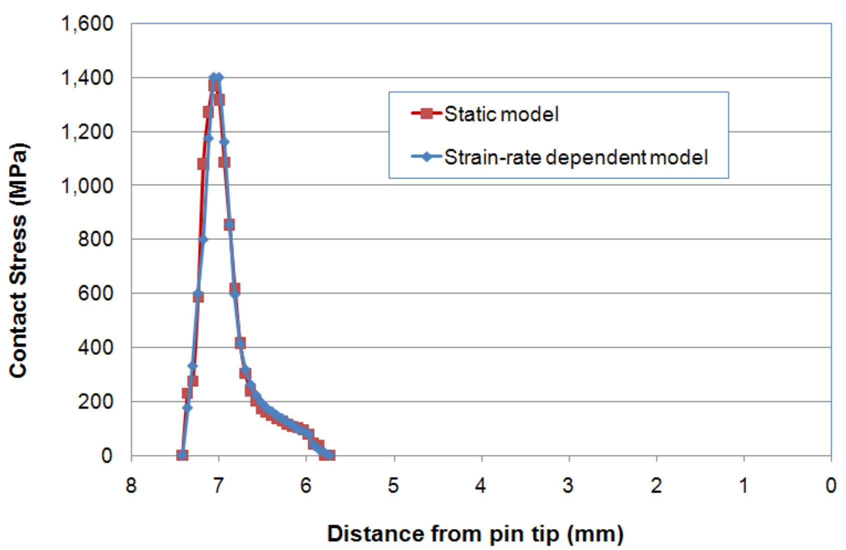

Figure 9. Distribution of seal contact stress after makeup based on static and strain-rate dependent models

5. Conclusions

This paper presents a discussion on the application and behaviour of the alternative approaches for modeling the makeup of premium tubular connection using static and strain-rate dependent material models. The static model assumed time-independent loading for the interference fit in the thread, seal and shoulder. The strain-rate dependent model considered the effect of yield strength increase due to the quick loading rate typical of oilfield connection makeup. An analysis example with a 244.5 mm, 59.5 kg/m Grade 80 generic premium connection was presented to demonstrate the behaviour of the proposed analysis models.

Based on the discussions and analyses presented in this paper, the following conclusions and recommendations are made:

- The static model appears to overestimate the magnitude of the plastic strain and the extent of the yield zone. As a result, the static model was unable to predict the primarily linear response of torque-turn relationship as observed in field and lab.
- The strain-rate dependent model showed a more limited yield zone with less plastic strain in the shoulder region, and it was able to capture the primarily linear response of torque-turn relationship.
- The seal contact profiles at the end of makeup were essentially equivalent for the two models and appeared not to be affected by the loading rate.

6. References

1. Abaqus Analysis User's Manual, version 6.10, 2010.
2. Manjoine, M. J. "Influence of Rate of Strain and Temperature on Yield Stresses of Mild Steel", Journal of Applied Mechanics, 11, A-211, (1944).
3. Marojevic, S. T. "Computer Control of Minimum Shoulder Prestress Requirements During Makeup Procedure of Premium Shoulder Connections", IADC/SPE 14793, 1986.
4. Raney, J. B., Lamb, J. F. "Running and Handling of a Premium Connection on a Rig", SPE/IADC 18698, 1989.
5. Stewart, A. A. "Controlled Make-up Procedures for Improved Workovers and Completions", SPE 16542, 1987.
6. TenarisHydril, "Make-up Acceptance Criteria", www.tenaris.com, 2011.
7. Tsuru, E., Maruyama, K., Inowaki, R., Tochikawa, T. "Allowable Torque of Tubular Connection under Simulated Running and Working Conditions", SEP/IADC 29353, 1995.
8. Weiner, P. D., Sewell, F. D. "New Technology for Improved Tubular Connection Performance", JPT, March 1967.
9. Willis, D. N. "How to Ensure Proper Make-up of Premium Shoulder Tubulars", World Oil, September, 1983.
10. Xie, J. "Analysis of Oil Well Casing Connections Subjected to Non-axisymmetric Loads", Abaqus Users' Conference, Paris, France, May 2007, pp. 634-646.
11. Xie, J. "Investigation of Casing Connection Failure Mechanisms in Thermal Wells", Paper 2009-353, World Heavy Oil Congress, Puerto La Cruz, Venezuela, November 2009.

12. Xie, J. and Tao, G., "Analysis of Casing Connections Subjected to Thermal Cycle Loading", Abaqus Users' Conference, RI, USA, May 2010, pp. 679-694.

7. Acknowledgement

The work summarized and the preparation of this paper was supported by C-FER Technologies, Canada. The author would like to sincerely acknowledge Dr. Gang Tao, Research Engineer, for his assistance in developing finite element models, Mr. Todd. A. Zahacy, Senior Engineering Advisor, Exploration and Production, C-FER Technologies, for his technical advice and assistance in preparing and reviewing this paper, and Dr. Chengye Fan, Research Engineer, for his assistance in the final technical review of this paper.